

Comparative Study of the Energy Transfer Kinetics in Artificial BChl *e* Aggregates Containing a BChl *a* Acceptor and BChl *e*-Containing Chlorosomes of *Chlorobium phaeobacteroides*

Burkhard Zietz,^{*,†} Valentin I. Prokhorenko,^{‡,#} Alfred R. Holzwarth,^{*,‡} and Tomas Gillbro[†]

Department of Chemistry, Biophysical Chemistry, Umeå University, SE-90187 Umeå, Sweden, and
Max-Planck-Institut für Bioanorganische Chemie, Stiftstrasse 34-36, D-45470 Mülheim a.d. Ruhr, Germany

Received: June 26, 2005; In Final Form: November 12, 2005

Chlorosomes are the light-harvesting organelles of green bacteria, containing mainly special bacteriochlorophylls (BChls) carrying a 3¹-hydroxy side chain. Artificial aggregates of BChl *c*, *d*, and *e* have been shown to resemble the native chlorosomes in many respects. They are therefore seen as good model systems for understanding the spectroscopic properties of these antenna systems. We have investigated the excitation energy transfer in artificial aggregates of BChl *e*, containing small amounts of BChl *a* as an energy acceptor, using steady-state and time-resolved fluorescence. Global analysis of the kinetic data yields two lifetimes attributable to energy transfer: a fast one of 12–20 ps and a slower one of ~50 ps. For comparison, BChl *e*-containing native chlorosomes of *Chlorobium phaeobacteroides* and chlorosomes in which the energy acceptor had been degraded by alkaline treatment were also studied. A similar behavior is seen in both the artificial and the natural systems. The results suggest that the artificial aggregates of BChls have a potential as antenna systems in future artificial photonic devices.

Introduction

Photosynthetic green sulfur bacteria are adapted to growth under very low light conditions. To utilize this scarce light as efficiently as possible, they have developed special antenna systems, so-called chlorosomes. These contain large amounts of bacteriochlorophyll (BChl) *c*, *d*, or *e* aggregates surrounded by a monolayer of glycolipids, mainly MGDG (monogalactosyl diglyceride) (see, e.g., refs 1–3 for reviews). It is now generally accepted that the structure of the chlorosomes is controlled by pigment–pigment interaction only, as first proposed by Bystrova et al.,⁴ although their original suggestion of a keto···magnesium and an OH···pyrrol nitrogen coordination is not realized in these supramolecular aggregate structures.^{5–7} Several different kinds of green bacterial BChl aggregates have been suggested in the literature (see, e.g., a recent review on self-aggregated chlorins⁸). A detailed aggregation and binding model giving rise to the tubular structures found in chlorosomes has been proposed by Holzwarth and Schaffner⁹ using molecular modeling based on the results from optical properties and extensive aggregation studies.^{7,10} This binding model has later been experimentally confirmed and extended using solid-state NMR.^{6,11–13} These data also confirmed the earlier suggestion^{10,14,15} of the identity of the aggregate organization in intact chlorosomes and in *in vitro* aggregates.^{6,7,10} Very recently, single tubular rod structures for aggregates of a semisynthetic BChl *d* analogue have been demonstrated using atomic force microscopy.¹⁶ However, Pšenčík et al. recently questioned the tubular rod structure of chlorosomes.¹⁷ Due to the close contact of the aggregated

chromophores, the spectroscopic properties of the chlorosomes and the artificial aggregates are dominated by exciton interactions.^{18,19} Here, in contrast to all other known antenna systems, proteins play only a minor role.^{1,8} They are not necessary for stabilization of the structure, as was shown biochemically by Holzwarth et al.²⁰ with chlorosomes and by preparation of artificial aggregates,^{7,21} which were devoid of proteins but showed strikingly similar absorbance and CD spectra (see also extensive review ref 8 for further references on artificial aggregates).

The unique properties of chlorosomes make them an interesting model for antenna systems in artificial photosynthesis.¹ The high energy transfer efficiency of such self-assembled artificial antennae incorporating an energy acceptor has been demonstrated by Tamiaki et al.²² and Prokhorenko et al.,²³ with efficiencies reaching 70%. Electron-transfer dyads, suitable for incorporation into chlorin-based self-assembled structures, have also been synthesized and characterized²⁴ and incorporated into artificial light-harvesting devices.²⁵

Attached to the native chlorosomes is a so-called base-plate, which contains BChl *a* associated with the CsmA protein in the chlorosomal envelope.²⁶ This complex mediates energy transfer from the chlorosomal BChl *c*, *d*, or *e* aggregates to the FMO (Fenna–Matthews–Olson) protein and/or the membrane-bound antenna complexes.⁸

The energy transfer processes in isolated chlorosomes and in whole cells have been the subject of many earlier studies, with the focus mainly on BChl *c*-containing species. For *Chloroflexus (Cfl.) aurantiacus*, an energy transfer component between the BChl *c* aggregates and the base-plate BChl *a* of 15–16 ps was found by several groups for whole cells^{27–29} and 8–11 ps for isolated chlorosomes.³⁰ Savikhin et al.³¹ reported two components of 2–3 and 11 ps, which, however, were not measured under reducing conditions, and therefore are likely

* Corresponding authors. E-mail: burkhard.zietz@chem.umu.se; holzwarth@mpi-muelheim.mpg.de.

[†] Umeå University.

[‡] Max-Planck-Institut für Bioanorganische Chemie.

[#] Present address: Department of Chemistry, University of Toronto, Canada, M5S 3H6.

to include quenching by oxidized BChl *c* radicals, as suggested by van Noort et al.³²

In a photon-echo study of the *C. aurantiacus*- and *Chlorobium* (*Chl.*) *tepidum*-isolated chlorosomes, performed at low temperature, the energy transfer between rod aggregates within the chlorosomes was also clarified, and a kinetic scheme for the energy transfer processes was proposed.^{18,19} For *Chl. vibrioforme*, energy-trapping times of ~45 ps for isolated chlorosomes and ~64 ps for whole cells have been reported,³³ although with a limited time resolution. In another study on the same species, identical energy transfer times of 66 ps for isolated chlorosomes and whole cells were obtained.²⁸ In chlorosomes from *Chl. limicola*, containing BChl *c* and BChl *d*, two energy transfer (ET) components to BChl *a* of 27 and 74 ps were found,³⁴ and, at low temperatures, an additional transfer component of 4 ps from BChl *d* to BChl *c* was resolved. Transient absorption studies on chlorosomes from the BChl *c*-containing species *Chl. tepidum* yielded ET times of 30–40 ps.³⁵

For the BChl *e*-containing species *Chl. phaeovibrioides* a time constant for energy trapping by BChl *a* of 60 ps was reported³⁶ using transient absorption spectroscopy under weakly reducing conditions (sodium ascorbate, but no sodium dithionite was used), which is comparable with the 56 ps component found for *Chl. phaeobacteroides* by fluorescence kinetics.³⁷ The latter study required only three lifetime components for fitting the whole spectral range of 750–820 nm. In a later study, comparing carotenoid-free chlorosomes with control chlorosomes, two lifetime components of ~30 and 90 ps for energy transfer to BChl *a* were resolved for carotenoid-containing (control) chlorosomes.³⁸

The time-correlated single-photon counting (SPT) technique is not able to resolve the fastest (subpicosecond) processes in the chlorosomes, but it can deliver very accurate data on the time scale starting from a few picoseconds, and it easily allows one to resolve the energy transfer steps from the artificial aggregate body to an attached energy trap.³⁹ We have now investigated the first steps in the energy transfer chain from BChl *e* to BChl *a* in artificial aggregates and in chlorosomes of *Chl. phaeobacteroides* using both time-resolved and steady-state fluorescence. The BChl *e*/BChl *a* system was chosen because of the especially good spectral overlap of BChl *e* aggregate emission and BChl *a* absorption, thus allowing for efficient energy transfer. Moreover, most previous studies have been carried out on BChl *c*-containing species, while little is known about energy transfer in BChl *e*-containing species.

Our study is aimed at answering the following questions:

- (1) Is an artificial self-assembled system, consisting of BChl *e*/BChl *a*/lipid, sufficient to mimic the main features of the light-harvesting apparatus of green bacteria?
- (2) Does the system meet the basic requirements for serving as a building block in artificial light-harvesting systems?
- (3) What are the optimal conditions for such devices (ratio of BChl *e*/BChl *a*, stabilization time, etc.)?

Materials and Methods

Sample Preparation. BChl *e* was purified by HPLC from an extract of whole cells of *Chl. phaeobacteroides*, collecting the main fraction, i.e., the one containing farnesyl ester side chains.⁴⁰ BChl *a* was obtained from *Rhodospirillum rubrum* extracts by HPLC and contained geranylgeraniol ester side chains.⁴¹ MGDG (95%) was purchased from Sigma. Aggregates of BChl *e* were prepared by the following procedure: Buffer (20 mM Tris–HCl, pH = 8.0) was first deaerated by bubbling with argon. To remove remaining traces of oxygen and to ensure

reducing conditions, a small amount of Na₂S₂O₄ solution was added. Sodium dithionite was added before aggregation to make sure that no oxygen is present inside the aggregates. In a separate vial, BChl *e* and MGDG (10 μg) were dissolved in 20 μL of methanol (MeOH) and injected under a stream of argon into ~3 mL of buffer, and the mixture was shaken vigorously. The pH was measured before and after fluorescence measurements to ensure a pH of at least 7.0 (NaHSO₃ formed by oxidation of sodium dithionite can lead to pheophytinization of BChl *e*). The final concentrations of MGDG and Na₂S₂O₄ were ~3.3 μg/mL and 3 mM, respectively. The aggregates were left to stabilize in the dark at room temperature overnight.

Chlorosomes were subjected to alkaline treatment according to the literature³⁷ in order to degrade the primary energy acceptor by adding 0.3 mL of 10 M NaOH to 3 mL of a suspension of chlorosomes in 10 mM potassium phosphate buffer (pH = 7), heating in a water bath to 40 °C for 20 min, and diluting with 1.0 M potassium phosphate buffer pH = 6 to get a final pH of 7.2.

In experiments involving chlorosomes, sodium dithionite was added at least 3 h before the measurements to stabilize fully reducing conditions.

Single-Photon Timing (SPT) Measurements. The laser system and SPT equipment used for experiments were described in detail elsewhere.³⁹ For the SPT measurements about 3 mL of a sample with an absorbance of ~1 cm⁻¹ at the excitation wavelength was used in a closed cuvette of 1 cm path length. To avoid possible photooxidation of the samples by molecular oxygen, all measurements were conducted under a nitrogen atmosphere in the presence of small amounts of sodium dithionite. Samples were excited with laser pulses (fwhm of 10 ps) at a repetition rate of 4 MHz. The excitation energy density was 2–4 × 10¹¹ photons/cm²/pulse. It was checked that no excitation annihilation occurs under these conditions. The system response was ~30 ps fwhm, allowing a resolution of lifetimes down to 3 ps by the deconvolution procedure. The decay traces were fitted using the global analysis method, resulting in decay-associated fluorescence spectra (DAS), i.e., a plot of the associated lifetime amplitudes $A(\lambda)_i$ versus wavelength:

$$D(t, \lambda) = P(t) \otimes \sum_i A(\lambda)_i \exp(-t/\tau_i)$$

where $D(t, \lambda)$ are decay traces measured at different wavelengths λ , $P(t)$ is the measured apparatus response function, τ_i are (fitted) lifetimes, and the symbol \otimes denotes a convolution integral.⁴²

Steady-State Spectroscopy. Absorption spectra were measured in a Shimadzu UV-1601 spectrophotometer (Japan) in a standard 1 cm fluorescence cell. Stationary fluorescence emission spectra were recorded using the above SPT equipment in steady-state mode and corrected for the wavelength-dependent sensitivity of the detection system.

Results

1. Artificial Aggregates. Upon aggregation, the Q_y absorption maximum of BChl *e* is shifted from 658 nm (for the monomer in MeOH) to between 700 and 720 nm (depending on the conditions of preparation and on the homologue distribution within the BChl; $Q_y(\text{max}) = 706$ nm in the aggregates used in our experiments). The red-shift is accompanied by a large rise in intensity of the Q_y band as compared to the Soret band (Figure 1a). In the presence of BChl *a* during aggregation, a shoulder occurs around 785 nm (Figure 1b). The spectral overlap between BChl *e* aggregate emission and BChl *a* absorption is demonstrated by the inset in Figure 1a, showing the difference in

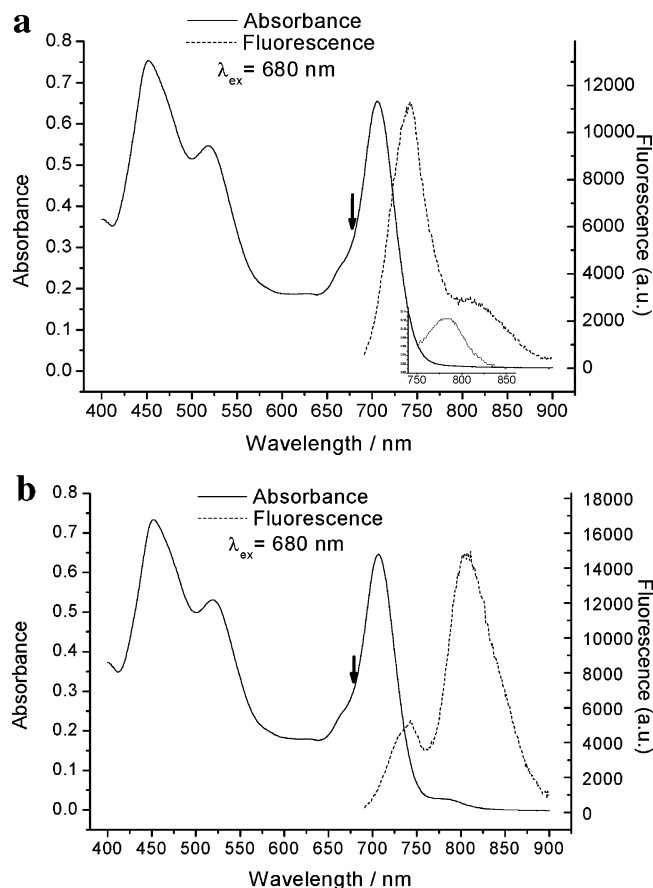


Figure 1. Absorption and steady-state fluorescence spectra of (a) BChl *e* aggregates and (b) coaggregates of BChl *e*/BChl *a* = 20:1; the arrows mark the wavelength of excitation. The inset in (a) shows the BChl *a* absorption spectrum in aggregates.

absorption between BChl *e* + BChl *a* coaggregates and BChl *e* aggregates. The observed absorption maximum for coaggregated BChl *a* is red-shifted by ca. 15 nm, as compared to that of BChl *a* in methanol solution.

Aggregates of BChl *e* show emission with a maximum at ~740 nm, corresponding to a Stokes shift of about 35 nm, and a shoulder between 800 and 880 nm (see Figure 1a). By adding a small amount of BChl *a* before aggregation, the steady-state fluorescence changes substantially. A new maximum at ~810 nm occurs and is slightly red-shifted against the red shoulder of the BChl *e* emission (Figure 1b).

1.1. Time-Resolved Fluorescence. Figure 2a shows the DAS of aggregates of BChl *e*, and Figure 2b shows the DAS of coaggregates of BChl *e* and BChl *a* (ratio 20:1), both excited at 680 nm. Four or five lifetime components are necessary to obtain a good fit in the global analysis.

1.1.1. Pure BChl *e* Aggregates. In the case of pure BChl *e* aggregates (Figure 2a), the fastest component of ~18 ps has a large positive amplitude around 725 nm, i.e., to the blue side of the steady-state fluorescence maximum. The DAS of the decay components of 89 and 164 ps resemble the steady-state emission spectrum. In the DAS of the long-lived component (455 ps), which has a minor amplitude only, two maxima, located at 740 nm and ≥840 nm, can be distinguished. In another experiment, the ~20 ps component showed a positive amplitude at shorter wavelengths (below 740 nm) and a small negative amplitude around 760 nm (data not shown).

1.1.2. BChl *e*/BChl *a* Coaggregates. The kinetics of coaggregates of BChl *e*/BChl *a* (Figure 2b) require 5 lifetime components. The two fast ones of 10–12 ps and 36–50 ps can

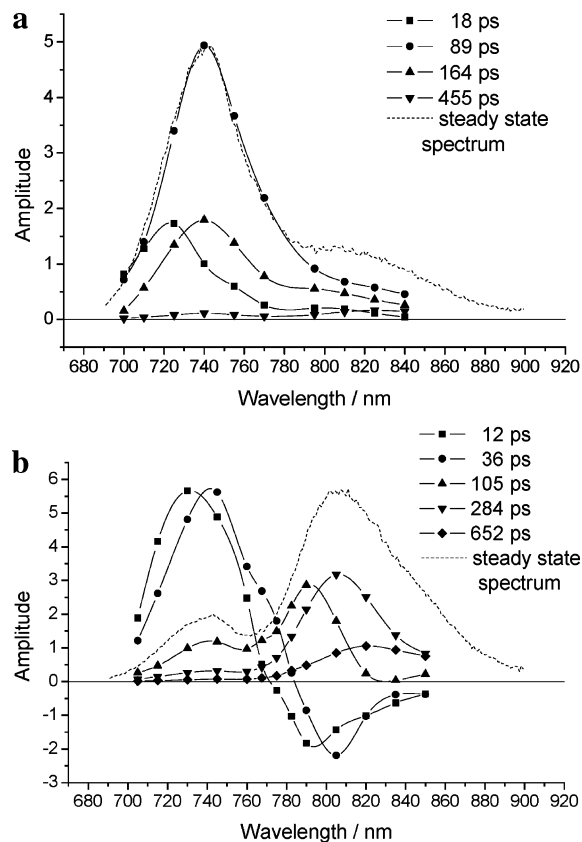


Figure 2. DAS of aggregates of (a) BChl *e* and (b) coaggregates of BChl *e* and BChl *a* (20:1).

be attributed to energy transfer processes (with positive amplitudes at shorter wavelengths and negative amplitudes at longer wavelengths). The shorter one is blue-shifted 10–20 nm as compared to the longer one. Moreover, the 36–50 ps component shows a shoulder at ~770 nm, which coincides with the zero-crossing point of the shortest lifetime component. The distribution of the positive and negative amplitudes matches quite well with the BChl *e* and BChl *a* emission spectra, respectively.

An intermediate component of ~100 ps shows a maximum at a wavelength that matches well with the blue-shifted minimum (790 nm) of the above-mentioned fastest 12 ps component. An ~280 ps component shows a positive peak at a wavelength corresponding to the red-shifted minimum (805 nm) of the 36 ps component. This is considered as evidence that two spectrally different kinds of energy acceptors are populated, which then also decay with slightly different lifetimes.

The slowest decaying component (~650 ps) has a positive amplitude at the long wavelength side with a maximum at 820 nm.

2. Chlorosomes. The DAS of several fluorescence components from chlorosomes (Figure 3, parts a and b) are centered within a narrower wavelength range than those of the artificial aggregates. All the shorter wavelength bands from both control and alkaline-treated chlorosomes are located at 740–750 nm, and the red emission is centered at 830 nm (shoulder) for alkaline-treated and 810 nm for control chlorosomes, respectively. For alkaline-treated chlorosomes, a fast decaying component is observed with ~12 ps lifetime, which has positive amplitudes between 710 and 800 nm and small negative amplitudes above 810 nm. The other four lifetime components show mainly the same features as the steady-state emission spectrum. However, the ~60 ps and the ~140 ps components are lower in intensity and the two longest-lived components

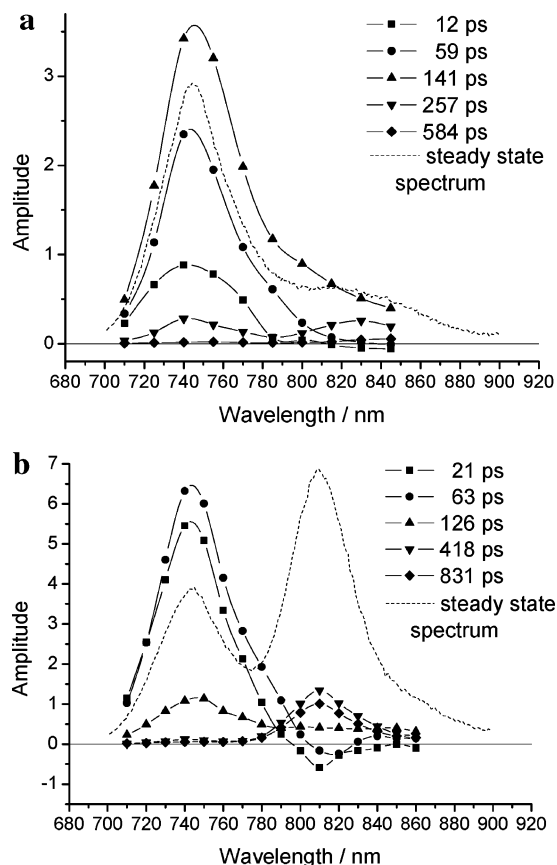


Figure 3. DAS of (a) alkaline-treated and (b) control chlorosomes.

are higher in intensity, above 800 nm, which is the emission corresponding to the red shoulder. Native control chlorosomes (Figure 3b) show two components with positive amplitudes between 710 and 800 nm and negative amplitudes between 800 and 840 nm. One intermediate lifetime component of ~ 125 ps shows a band peaking at ~ 750 nm and a long tail extending to 850 nm. The two longest components are nearly exclusively emitting from the wavelength region above 800 nm, closely matching the emission from BChl *a*.

Discussion

Artificial Aggregates. The unusually large Stokes shift of ~ 35 nm (~ 680 cm^{-1}) between absorbance and fluorescence in aggregates of BChl *e* can be explained by low-energy excitonic bands having small oscillator strength¹⁸ and therefore not contributing significantly to the absorption. However, they can be effectively populated from higher excitonic levels within several hundreds of femtoseconds up to a few picoseconds.¹⁹ Due to the relatively large energy splitting between these “terminal” exciton states and the higher exciton levels, the excitation energy will be trapped on the low-lying states in the long-lived emission with decay time(s) of 500–1000 ps. The shoulder in the emission spectrum, extending to about 880 nm, is most likely due to contributions from molecular vibrational states. The 18 ps component reflects emission from the higher exciton states which relax to the lower exciton states. However, the expected negative amplitude at long wavelengths of this component is only very small due to the very similar emission spectra of the different states, which makes its detection very difficult in this overall complex kinetics (see above). Emission from several different exciton states with different lifetimes due to different radiative rates but similar emission spectra has been reported earlier.²³ It cannot be excluded, furthermore, that part

of this heterogeneous fluorescence is also caused by a mixture of different sizes of aggregates as discussed.²³ The 725 nm emitting species with small amplitude (Figure 2a) may be due to a very low-lying exciton state with small radiative rate. Without precise knowledge of the structure and size distribution of these aggregates these interpretations have to be taken, however, with a grain of salt.

In the coaggregates containing BChl *a*, the two fast lifetime components (of 10–15 ps and 25–50 ps) reflect the energy transfer from the BChl *e* aggregate body to the BChl *a* energy trap. The negative component in the DAS overlaps the BChl *a* emission spectrum, corresponding to the rise time in the emission from BChl *a*. Chlorosomes show two similar components, but with somewhat longer lifetimes (~ 25 and 70 ps). Assuming that the supramolecular aggregation of the BChl *e* molecules is not considerably distorted by the small amount of intertwined BChl *a* energy acceptors, similar processes are expected to occur in coaggregates containing BChl *e*/BChl *a* as in pure BChl *e* aggregates. There seem to exist two different terminal emitters, having maxima around 800 and 820 nm and different lifetimes. They also differ in the species and lifetimes of the BChl *e* aggregates from which they are sensitized. We tentatively assign these two emitters to be present in different aggregates which may differ either in size or in the type of binding of BChl *a* to the aggregates. At present, it is not possible to decide between these possibilities. We also note that a five component analysis probably just is a minimal description of the true kinetics. Considering the overall complexity of the system, it would not be surprising if not all processes can be resolved by fitting with five components. Previously, the energy transfer processes within pure BChl *e* aggregates have been resolved with higher resolution by femtosecond pump–probe absorption spectroscopy.⁴³ Two important differences between the coaggregates and intact chlorosomes have to be kept in mind: first, in chlorosomes the energy acceptor is located outside the chlorosomal aggregates in the so-called base-plate, which can explain the substantially longer ET times, and second, our artificial coaggregates contain no carotenoids, in contrast to natural chlorosomes. Moreover, little is known about how exactly the BChl *a* is embedded in the coaggregates. From previous studies, it has been concluded that the BChl *a* or BPhoe *a* trap replaces a chlorin molecule in the aggregates structure.²³ Our present measurements do suggest that there exist at least two different kinds of energy acceptors, which show a difference in emission wavelength of about 10 nm and a difference of energy-trapping rates of a factor of ~ 3 . One could speculate that these correspond to energy acceptors located more at the periphery and more in the center of the rods.

Chlorosomes. Chlorosomes are expected to be more uniform in their structure as compared to artificial aggregates, which is expressed in narrower emission bands for all the different components. Both base-plate-containing and base-plate-free chlorosomes show only one maximum between 700 and 780 nm, peaking at 740–745 nm for all of their DAS components (Figure 3, parts a and b). This emission can clearly be attributed to the BChl *e* rods. In intact control chlorosomes the minimum in the DAS of the shortest-lived component and the maxima of the three long-lived DAS components are centered at ~ 810 nm, matching the steady-state emission band of aggregated BChl *a*. However, the ~ 60 ps component has its minimum shifted to longer wavelengths. The two fast components (20–30 and 60–80 ps) are clearly identified as energy transfer components, possessing large positive bands corresponding to BChl *e* and small negative bands corresponding to BChl *a* emission. This

matches well with the results of Pšenčík et al.,³⁸ who determined ET times of ~ 30 and 90 ps for chlorosomes from the *Chl. phaeobacteroides* strain CL1401. It is interesting to note the 830 nm emitting species of 257 ps lifetime in trap-depleted chlorosomes (Figure 3a), which also emits with a second band at 740 nm. This is clearly not a BChl *a* emission band, as can be seen from comparison with Figure 3b. We assign this species to a similar origin as the analogous species in pure BChl *e* aggregates (Figure 2a) with a lifetime of 455 ps, i.e., most likely a very low-lying exciton transition with a low radiative rate. We speculate that it might possibly arise from some disturbance or defect in a regular chlorosomal-type rod element.

The fact that the emission of artificial aggregates is spread over a larger wavelength range can be understood by assuming aggregate fragments of different size, compared to larger and more homogeneous building blocks being present in chlorosomes. However, even the natural chlorosomes (Figure 3b) seem to contain two different energy acceptors that are reached by different pathways and lifetimes. We cannot come to a final assignment in this matter as long as the structure of the chlorosomal base-plate and the exact geometrical relation between base-plate BChls and chlorosome body is not clarified. Balaban et al. described the autocatalytic nature of the aggregation process of BChl *c* in nonpolar solvents.⁵ Assuming that a similar process takes place for BChl *e* in water/MGDG, it is plausible to expect a range of sizes for the aggregates, which in turn are expected to have slightly different spectroscopic properties, lifetimes, radiative rates, etc.

In experiments involving BChl *a* as energy acceptor, a noticeable decrease in emission from BChl *a* was seen after several hours of illumination, whereas the BChl *e* aggregate emission was unchanged even after several days. This is noteworthy in terms of photoprotection-aggregated BChl *e* does not seem to need photoprotection in contrast to BChl *a*. Therefore it is reasonable to assume that at least some of the carotenoids present in intact chlorosomes are in proximity to the BChl *a* acceptor, which is likely to be embedded in the CsmA protein.

Estimation of the Degree of Excitation Delocalization. With the use of the same approach as recently published in ref 23, the degree of delocalization can be estimated as the ratio of positive/negative amplitude in the DAS corresponding to the energy transfer process(es). This ratio reflects that between the radiative rates for the excited donor (BChl *e* aggregate) and the energy acceptor (a BChl *a* molecule). For the investigated artificial coaggregates, the degree of delocalization (in other words, the number of coherently coupled molecules in the aggregates), can be estimated to be ~ 3 for both observed energy transfer components. It should be pointed out that for the BChl *d*-based coaggregates, investigated in ref 23, delocalization occurs over at least 10 molecules, whereas for the zinc-chlorin-based coaggregates the delocalization number is ≈ 20 . For control chlorosomes (Figure 3b) this estimation cannot be made correctly, since the structural arrangement of the BChl *a*-containing base-plate is still unknown. However, the lowest limit of delocalization can be estimated if we assume that the dipole strength (and corresponding pure radiative rate) is the same as for free monomeric BChl *a* molecules. In that case, excitation in chlorosomes should be delocalized over at least 10 BChl *e* molecules. If the radiative emission rate constant for the base-plate is higher (e.g., due to exciton interaction of BChls within the base-plate), the degree of delocalization will be also correspondingly higher.

The energy transfer efficiency from the BChl *e* aggregates in both natural chlorosomes and artificial aggregates to the BChl *a* energy traps is very high, approaching 100%, as can be estimated from the relative amplitudes of positive and negative components in the region above 800 nm. Nevertheless, the fluorescence yield of both the artificial aggregates and of chlorosomes is relatively low. This is due to efficient quenching processes occurring in both systems within the BChl *e* part. This quenching is favored by the fact that a transfer equilibrium between BChl *e* and BChl *a* is reached within the excited-state lifetime of the system. It is important to note here, however, that this quenching is much less relevant in intact cells of green bacteria or in a hypothetical artificial system where the excitation energy is trapped by an electron-transfer process. Under such conditions, the average decay time of BChl *e* is much shorter (typically 40–60 ps in green sulfur bacterial cells and even shorter for cells of green nonsulfur bacteria) and no transfer equilibrium is reached. Thus, the sensitizing efficiency of chlorosomes in intact cells, and for a possible artificial system using the artificial aggregates with energy trap, can still reach very high values, above 90%, as is well-known from studies of intact green bacteria.

Conclusions

Using BChl *e*, MGDG, and BChl *a* in aqueous phase, we have been able to build the simplest working model of an artificial antenna system which is capable of fulfilling its main function, i.e., absorbing light and efficiently transferring it to the energy acceptor. The aggregation is, however, a random process, probably leading to a range of aggregate sizes, and thus the trapped energy is not collected in a well-defined, unique location. Nevertheless, we consider such artificial aggregates, containing a small amount of an energy acceptor, as suitable systems for use in artificial light-harvesting devices.

Acknowledgment. C. M. Borrego is gratefully acknowledged for providing the BChl *e* and M. Miller, Odense, for providing a sample of chlorosomes of *Chl. phaeobacteroides*. This work was supported in part by the EU TMR Network Project "Green Bacterial Photosynthesis" (Grant No. FMRX-CT96-0081).

References and Notes

- Holzwarth, A. R. Light Absorption and Harvesting. In *Molecular to Global Photosynthesis*; Archer, M. D., Barber, J., Eds.; Imperial College Press: London, 2004; pp 43–115.
- Olson, J. M. Green Bacteria: The Light-Harvesting Chlorosome. In *Encyclopedia of Biological Chemistry*; Lennarz, W. J., Lane, M. D., Eds.; Elsevier: Oxford, U.K., 2004; Vol. 2, pp 325–330.
- Olson, J. M. *Photochem. Photobiol.* **1998**, *67*, 61–75.
- Bystrova, M. I.; Mal'gosheva, I. N.; Krasnovskii, A. A. *Mol. Biol.* **1979**, *13*, 440–451.
- Balaban, T. S.; Leitich, J.; Holzwarth, A. R.; Schaffner, K. *J. Phys. Chem. B* **2000**, *104*, 1362–1372.
- Balaban, T. S.; Holzwarth, A. R.; Schaffner, K.; Boender, G. J.; de Groot, H. J. M. *Biochemistry* **1995**, *34*, 15259–15266.
- Chiefari, J.; Griebenow, K.; Fages, F.; Griebenow, N.; Balaban, T. S.; Holzwarth, A. R.; Schaffner, K. *J. Phys. Chem.* **1995**, *99*, 1357–1365.
- Balaban, T. S.; Tamiaki, H.; Holzwarth, A. R.; Chlorins programmed for self-assembly. In *Topics in Current Chemistry* 238; Springer-Verlag: Berlin, 2005; pp 1–38.
- Holzwarth, A. R.; Schaffner, K. *Photosynth. Res.* **1994**, *41*, 225–233.
- Hildebrandt, P.; Griebenow, K.; Holzwarth, A. R.; Schaffner, K. *Z. Naturforsch., C: Biosci.* **1991**, *46*, 228–232.
- van Rossum, B.-J.; Steensgaard, D. B.; Mulder, F. M.; Boender, G.-J.; Schaffner, K.; Holzwarth, A. R.; de Groot, H. J. M. *Biochemistry* **2001**, *40*, 1587–1595.

- (12) de Boer, I.; Matysik, J.; Erkelens, K.; Sasaki, S.; Miyatake, T.; Yagai, S.; Tamiaki, H.; Holzwarth, A. R.; de Groot, H. J. M. *J. Phys. Chem. B* **2004**, *108*, 16556–16566.
- (13) de Boer, I.; Matysik, J.; Amakawa, M.; Yagai, S.; Tamiaki, H.; Holzwarth, A. R.; de Groot, H. J. M. *J. Am. Chem. Soc.* **2003**, *125*, 13374–13375.
- (14) Holzwarth, A. R.; Griebenow, K.; Schaffner, K. Z. *Naturforsch., C: Biosci.* **1990**, *45*, 203–206.
- (15) Griebenow, K.; Holzwarth, A. R. *Biochim. Biophys. Acta* **1989**, *973*, 235–240.
- (16) Huber, V.; Katterle, M.; Lysetska, M.; Würthner, F. *Angew. Chem., Int. Ed.* **2005**, *44* (20), 3147–3151.
- (17) Pšenčík, J.; Ikonen, T. P.; Laurinmaki, P.; Merckel, M. C.; Butcher, S. J.; Serimaa, R. E.; Tuma, R. *Biophys. J.* **2004**, *87* (2), 1165–1172.
- (18) Prokhorenko, V. I.; Steensgaard, D. B.; Holzwarth, A. R. *Biophys. J.* **2003**, *85* (5), 3173–3186.
- (19) Prokhorenko, V. I.; Steensgaard, D. B.; Holzwarth, A. R. *Biophys. J.* **2000**, *79* (4), 2105–2120.
- (20) Holzwarth, A. R.; Griebenow, K.; Schaffner, K. Z. *Naturforsch., C: Biosci.* **1990**, *45*, 35–38.
- (21) Müller, M.; Gillbro, T.; Olson, J. M. *Photochem. Photobiol.* **1993**, *57* (1), 98–102.
- (22) Tamiaki, H.; Miyatake, T.; Rikukei, T.; Holzwarth, A. R.; Schaffner, K. *Angew. Chem., Int. Ed. Engl.* **1996**, *35* (7), 772–774.
- (23) Prokhorenko, V. I.; Holzwarth, A. R.; Müller, M. G.; Schaffner, K.; Miyatake, T.; Tamiaki, H. *J. Phys. Chem. B* **2002**, *106*, 5761–5768.
- (24) Holzwarth, A. R.; Katterle, M.; Müller, M. G.; Ma, Y.-Z.; Prokhorenko, V. *Pure Appl. Chem.* **2001**, *73* (3), 469–474.
- (25) Müller, M. G.; Katterle, M.; Prokhorenko, V.; Holzwarth, A. R. From aggregates and electron-transfer dyads to artificial photosynthetic units. Proceedings of the EMBO Workshop on Green and Heliobacteria; Holzwarth, A. R., Ed.; Passau, Germany, April 19–24, 2002.
- (26) Sakuragi, Y.; Frigaard, N.-U.; Shimada, K.; Matsuura, K. *Biochim. Biophys. Acta* **1999**, *1413*, 172–180.
- (27) Mimuro, M.; Nishimura, Y.; Yamazaki, I.; Kobayashi, M.; Wang, Z. Y.; Nozawa, T.; Shimada, K.; Matsuura, K. *Photosynth. Res.* **1996**, *48*, 263–270.
- (28) Causgrove, T. P.; Brune, D. C.; Wang, J.; Wittmershaus, B. P.; Blankenship, R. E. *Photosynth. Res.* **1990**, *26*, 39–48.
- (29) Müller, M. G.; Griebenow, K.; Holzwarth, A. R. *Biochim. Biophys. Acta* **1993**, *1144*, 161–169.
- (30) Holzwarth, A. R.; Müller, M. G.; Griebenow, K. *J. Photochem. Photobiol., B* **1990**, *5*, 457–465.
- (31) Savikhin, S.; Zhu, Y.; Blankenship, R. E.; Struve, W. S. *J. Phys. Chem.* **1996**, *100*, 3320–3322.
- (32) van Noort, P. I.; Zhu, Y.; LoBrutto, R.; Blankenship, R. E. *Biophys. J.* **1997**, *72*, 316–325.
- (33) Blankenship, R. E.; Wang, J.; Causgrove, T. P.; Brune, D. C. *Curr. Res. Photosynth.* **1990**, *2*, 17–24.
- (34) Steensgaard, D. B.; van Walree, C. A.; Permentier, H.; Baneras, L.; Borrego, C.; Garcia-Gil, J.; Aartsma, T. J.; Amesz, J.; Holzwarth, A. R. *Biochim. Biophys. Acta* **2000**, *1457*, 71–80.
- (35) Pšenčík, J.; Polívka, T.; Měmce, P.; Dian, J.; Kudrna, J.; Malý, P.; Hála, J. *J. Phys. Chem. A* **1998**, *102*, 4392–4398.
- (36) van Noort, P. I.; Francke, C.; Schoumans, N.; Otte, S. C. M.; Aartsma, T. J.; Amesz, J. *Photosynth. Res.* **1994**, *41*, 193–203.
- (37) van Walree, C. A.; Sakuragi, Y.; Steensgaard, D. B.; Böisinger, C. S.; Frigaard, N.-U.; Cox, R. P.; Holzwarth, A. R.; Müller, M. *Photochem. Photobiol.* **1999**, *69* (3), 322–328.
- (38) Pšenčík, J.; Ma, Y.-Z.; Arellano, J. B.; Garcia-Gil, J.; Holzwarth, A. R.; Gillbro, T. *Photosynth. Res.* **2002**, *71*, 5–18.
- (39) Prokhorenko, V. I.; Holzwarth, A. R.; Müller, M. G.; Schaffner, K.; Miyatake, T.; Tamiaki, H. *J. Phys. Chem. B* **2002**, *106*, 5761–5768.
- (40) Arellano, J. B.; Pšenčík, J.; Borrego, C. M.; Ma, Y.-Z.; Guyoneud, R.; Garcia-Gil, J.; Gillbro, T. *Photochem. Photobiol.* **2000**, *71* (6), 715–723.
- (41) Katz, J. J.; Strain, H. H.; Harkness, A. L.; Studier, M. H.; Svec, W. A.; Janson, T. R.; Cope, B. T. *J. Am. Chem. Soc.* **1972**, *94* (22), 7938–7939.
- (42) Holzwarth, A. R. Data analysis of time-resolved measurements. In *Biophysical Techniques in Photosynthesis*; Amesz, J., Hoff, A. J., Eds.; Advances in Photosynthesis Research; Kluwer Academic Publishers: Dordrecht, The Netherlands, 1996; pp 75–92.
- (43) Pšenčík, J.; Ma, Y. Z.; Arellano, J. B.; Hala, J.; Gillbro, T. *Biophys. J.* **2003**, *84* (2), 1161–1179.